ELSEVIER

Journal of Organometallic Chemistry 568 (1998) 213–223

Journal of Organometallic Chemistry

Triphenylstibine substituted manganese and rhenium carbonyls: synthesis and multinuclear NMR spectroscopic studies. X-ray crystal structures of *ax*-$[Mn_2(CO)_9(SbPh_3)]$, $[Mn(CO)_5(SbPh_3)][CF_3SO_3]$ and *fac*-$[Re(CO)_3Cl(SbPh_3)_2]$

Nicholas J. Holmes, William Levason *, Michael Webster

Department of Chemistry, University of Southampton, Southampton SO17 1BJ, UK

Received 1 May 1998

Abstract

The syntheses of $[Mn_2(CO)_{10-x}(SbPh_3)_x]$ ($x = 1$ or 2), $[Re_2(CO)_9(SbPh_3)]$, $[Mn(CO)_5(SbPh_3)][CF_3SO_3]$, $[M(CO)_4Cl(SbPh_3)]$, *fac*-$[M(CO)_3Cl(SbPh_3)_2]$ (M = Mn or Re) and *mer,trans*-$[Mn(CO)_3Cl(SbPh_3)_2]$ are reported. The complexes have been characterised by chemical analysis, IR and multinuclear NMR (^1H, $^{13}C\{^1H\}$ and ^{55}Mn) spectroscopies, and FAB mass spectrometry. The crystal structure of $[Mn_2(CO)_9(SbPh_3)]$ established the axial position of the $SbPh_3$ ligand (Mn–Sb 2.525(1), Mn–Mn 2.909(1) Å) and that of $[Mn(CO)_5(SbPh_3)][CF_3SO_3]$ confirmed the cation structure (Mn–Sb 2.596(3) Å). The crystal structure of *fac*-$[Re(CO)_3Cl(SbPh_3)_2]$ establishes the stereochemistry (Re–Sb 2.726(1), 2.729(2) Å). Differences in the products/isomers produced in reactions of $[M_2(CO)_{10}]$ and $[M(CO)_5Cl]$ with $SbPh_3$ and with the corresponding PR_3 and AsR_3 ligands are identified and discussed. © 1998 Elsevier Science S.A. All rights reserved.

Keywords: Manganese; Rhenium; Carbonyl; Stibine; X-ray structure

---

1. Introduction

Thermal or photochemical reaction of $[Mn_2(CO)_{10}]$ with phosphine or arsine ligands leads to $[Mn_2(CO)_{10-x}L_x]$ ($L = PR_3$ or AsR_3, $x = 1$ or 2) [1]. Reports of paramagnetic monomers $[Mn(CO)_4(PR_3)]$ formed in the thermal reactions [2] were not confirmed by subsequent workers [3–6] who identified the products as $[Mn_2(CO)_{10-x}(PR_3)_x]$ or $[HMn(CO)_4(PR_3)]$ and attributed the paramagnetism of some samples to impurities. 17e radicals $[Mn(CO)_4(PR_3)]$ which recombine very rapidly, are formed by flash photolysis of the dinuclear complexes in solution at low temperatures [7]. The brief mention [2] of the product of the thermal reaction between $[Mn_2(CO)_{10}]$ and $SbPh_3$ as the paramagnetic $[Mn(CO)_4(SbPh_3)]$ is thus open to considerable doubt. Apart from an orange $[Mn_2(CO)_8(SbPh_3)_2]$ mentioned in a preliminary communication as a decomposition product of $[HMn(CO)_4(SbPh_3)]$ [8], the stibine complexes have not been re-examined. Reports of tertiary stibine complexes of rhenium carbonyls are even rarer, and the only characterised complexes appear to be the carbonyl iodides $[Re(CO)_nI(SbPh_3)_m]$ ($n = 4$, $m = 1$; $n = 3$, $m = 2$) [1]. Our interest in these complexes arose for two reasons: firstly in connection with our recent studies of distibinomethane complexes of manganese [9], and secondly as models for comparison with BiR_3 complexes which we are currently investigating. We report here the synthesis and structural characterisation of some $SbPh_3$ complexes with both manganese and rhenium carbonyls.

---

* Corresponding author. Tel.: +44 1703 595000; fax: +44 1703 593782; e-mail: wxl@soton.ac.uk

0022-328X/98/$19.00 © 1998 Elsevier Science S.A. All rights reserved.
PII S0022-328X(98)00763-3

2. Results and discussion

We have previously found [9] that $Ph_2SbCH_2SbPh_2$ does not react at all easily with $[Mn_2(CO)_{10}]$ in high-boiling solvents, and thus we sought alternative synthetic routes. The reaction of $[Mn_2(CO)_{10}]$ with $SbPh_3$ and Me_3NO (1:1.15:1 mol ratio) in toluene, followed by removal of the solvent, and chromatography on silica eluting with *n*-hexane produced unchanged $[Mn_2(CO)_{10}]$ and moderate yields (10–15%) of orange-brown $[Mn_2(CO)_9(SbPh_3)]$. Use of a larger excess of $SbPh_3$ and Me_3NO increased the proportion of the monosubstituted complex, but did not produce the expected disubstitution. Photolysis of a mixture of $[Mn_2(CO)_{10}]$ and $SbPh_3$ (1:2 mol ratio) in toluene (12 h, 370 nm) produced a dark-red solution and some black solid. Filtration, evaporation of the filtrate to dryness, and chromatography on silica (*n*-hexane), gave three main products, in addition to some dark orange material which did not elute. The complexes were identified in order of elution as $[Mn_2(CO)_{10}]$, $[Mn_2(CO)_9(SbPh_3)]$, and deep orange-yellow $[Mn_2(CO)_8(SbPh_3)_2]$.

The identification of the $[Mn_2(CO)_9(SbPh_3)]$ complex as the axial-substituted isomer (*I*) followed from the presence of five CO stretching modes in its IR spectrum [10], and this was confirmed by an X-ray study. The $^{13}C\{^1H\}$ NMR spectrum showed only two carbonyl resonances, a weak one due to the unique axial CO group and a much stronger one due to the eight equatorial CO's. The failure to resolve two resonances corresponding to the equatorial carbonyl groups in the $-Mn(CO)_5$ and the $-Mn(CO)_4(SbPh_3)$ residues is attributable to their very similar environments and the line broadening produced by the ^{55}Mn quadrupole moment [11]. The identification of the two manganese centres by ^{55}Mn NMR spectroscopy (Table 2) is notable and is discussed below.

The structure consists of discrete molecules based on the $[Mn_2(CO)_{10}]$ structure with an axially substituted $SbPh_3$ ligand (Fig. 1). The Mn–Mn distance (2.909(1) Å) can be compared with the parent carbonyl (2.9038(6) ([12]a) and 2.8950(6) Å ([12]b)) and a similar axially substituted phosphine (PMe_2Ph) derivative (2.904(–) Å) [13]. Both of these compounds and the present one show Mn–Mn–C angles less than 90° as the equatorial CO's bend towards the Mn–Mn bond, and with the two $Mn(CO)_4$ groups staggered (a typical torsion angle C(1)–Mn(1)–Mn(2)–C(5) in the present compound is 44.5(3)°). The axial CO on Mn(2) has a significantly shorter Mn–C bond than the eight equatorial Mn–C distances (Table 1). Few Mn–Sb bonds have been characterised crystallographically and none with $SbPh_3$.

The orange-yellow $[Mn_2(CO)_8(SbPh_3)_2]$ was identified as the diaxial isomer (*II*) since it shows only one broad CO stretch in the IR spectrum (1977 cm^{-1}) whereas ax–eq or eq–eq substitution produces more complex IR absorption patterns in the CO region [10]. The $^{13}C\{^1H\}$ NMR spectrum contains a single δ(CO) resonance consistent with the diaxial isomer, although due to the line broadening caused by the ^{55}Mn nuclei in other systems, this result is not conclusive in isolation. The compound differs from that mentioned [8] as a decomposition product of $[HMn(CO)_4(SbPh_3)]$ (ν(CO): 2062, 2010, 1980, 1953, 1825 cm^{-1}), which may have been an eq,eq isomer (full characterisation was not provided). We note that $[Mn_2(CO)_8(PR_3)_2]$ ($R_3 = Et_3$, $PhMe_2$) are diaxial isomers, whereas $[Mn_2(CO)_8(AsR_3)_2]$ ($R_3 = Et_3$, $PhMe_2$, Me_3) are diequatorial isomers, although $[Mn_2(CO)_8(AsPh_3)_2]$ is again a diaxial form [10]. Finally we re-examined the thermal reaction of $[Mn_2(CO)_{10}]$ with $SbPh_3$ in boiling *o*-xylene (12 h). Most of the starting materials were recovered unchanged, along with some insoluble brown material, and a very small amount of orange solid which had ν(CO) at 2013(m), 1998(m), 1968(s) cm^{-1}. These frequencies do not correspond to those of $[Mn_2(CO)_{10-x}(SbPh_3)_x]$ ($x = 1$ or 2), nor those of $[HMn(CO)_4(SbPh_3)]$ [8], and due to the very poor yields the material was not further characterised.

Photolysis of a mixture of $[Re_2(CO)_{10}]$ and $SbPh_3$ (1:2 mol ratio) in toluene was carried out in a similar way to the reaction with $[Mn_2(CO)_{10}]$. Chromatography using *n*-hexane–CH_2Cl_2 as elutant separated unchanged $[Re_2(CO)_{10}]$ and a yellow solid identified as $[Re_2(CO)_9(SbPh_3)]$. Under these conditions, and in contrast to the manganese chemistry, and to $[Re_2(CO)_{10}]/PR_3$ reactions [1], there was no evidence for disubstitution. The $[Re_2(CO)_9(SbPh_3)]$ was identified as the axial isomer [14] by IR spectroscopy (ν(CO) (CH_2Cl_2): 2086, 2008, 1994, 1978, 1925 cm^{-1}), a very

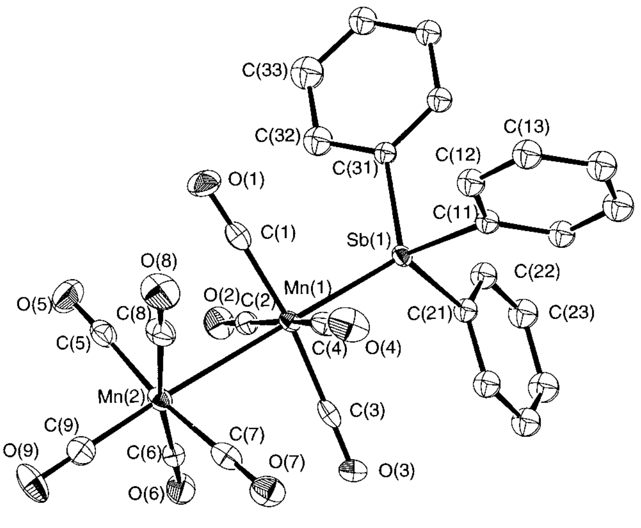

Fig. 1. Molecular structure of $[Mn_2(CO)_9(SbPh_3)]$ showing the atom labeling scheme. Displacement ellipsoids are drawn at the 50% probability level.

Table 1
Selected bond lengths (Å) and angles (°) for [$Mn_2(CO)_9(SbPh_3)$], [$Mn(CO)_5(SbPh_3)$][CF_3SO_3] and [$Re(CO)_3Cl(SbPh_3)_2$]

(a) [$Mn_2(CO)_9(SbPh_3)$]			
Mn(1)–Sb(1)	2.525(1)	Sb(1)–C(11)	2.164(7)
Mn(1)–Mn(2)	2.909(1)	Sb(1)–C(21)	2.146(6)
Mn(2)–C(9)	1.824(8)	Sb(1)–C(31)	2.146(6)
Mn–C (not C(9))	1.857(7)–1.884(8)		
C–O	1.128(8)–1.166(8)		
C–C	1.39(1)–1.42(1)		
Mn(1)–Sb(1)–C(11)	121.1(2)	C(11)–Sb(1)–C(21)	99.9(2)
Mn(1)–Sb(1)–C(21)	117.2(2)	C(11)–Sb(1)–C(31)	98.6(2)
Mn(1)–Sb(1)–C(31)	116.9(2)	C(21)–Sb(1)–C(31)	99.2(2)
Mn(2)–Mn(1)–Sb(1)	178.06(4)		
Mn(1)–Mn(2)–C (ca. 90°)	84.1(2)–88.2(2)		
Mn(2)–Mn(1)–C	85.4(2)–89.2(2)		
Sb(1)–Mn(1)–C	92.4(2)–94.7(2)		
Mn–C–O	177.2(6)–179.9(7)		
(b) [$Mn(CO)_5(SbPh_3)$][CF_3SO_3]			
Mn(1)–Sb(1)	2.596(3)	Sb(1)–C(11)	2.128(7)
Sb(1)–C(21)	2.129(7)	Mn(1)–C(5)	1.824(8)
Sb(1)–C(31)	2.118(7)		
Mn–C (not C(5))	1.874(8)–1.890(8)		
C–O	1.119(9)–1.139(8)		
C–C	1.36(1)–1.41(1)		
Mn(1)–Sb(1)–C(11)	117.9(2)	C(11)–Sb(1)–C(21)	101.0(3)
Mn(1)–Sb(1)–C(21)	115.2(2)	C(11)–Sb(1)–C(31)	105.4(3)
Mn(1)–Sb(1)–C(31)	112.6(2)	C(21)–Sb(1)–C(31)	102.9(3)
Sb(1)–Mn(1)–C(5)	176.5(2)		
Sb(1)–Mn(1)–C (ca. 90°)	85.1(2)–91.6(2), (88.6(av))		
Mn–C–O	176.4(7)–178.5(6)		
(c) [$Re(CO)_3Cl(SbPh_3)_2$]			
Re–Sb(1)	2.729(2)	Re–C(1)	1.95(1)
Re–Sb(2)	2.726(1)	Re–C(2)	1.97(1)
Re–Cl	2.504(3)	Re–C(3)	1.92(1)
Sb(1)–C(11)	2.12(1)	Sb(2)–C(41)	2.15(1)
Sb(1)–C(21)	2.12(1)	Sb(2)–C(51)	2.12(1)
Sb(1)–C(31)	2.14(1)	Sb(2)–C(61)	2.17(1)
C–O	1.06(1)–1.16(1)		
C–C	1.34(2)–1.42(2)		
Sb(1)–Re–Sb(2)	95.73(3)	C(1)–Re–C(2)	92.3(4)
Sb(1)–Re–Cl	88.67(8)	C(1)–Re–C(3)	88.8(4)
Sb(2)–Re–Cl	84.24(7)	C(2)–Re–C(3)	89.1(4)
Sb(1)–Re–C(3)	178.2(3)	Cl–Re–C(2)	174.5(3)
Sb(2)–Re–C(1)	173.8(3)		
Re–Sb(1)–C(11)	122.0(3)	Re–Sb(2)–C(41)	114.1(3)
Re–Sb(1)–C(21)	113.3(3)	Re–Sb(2)–C(51)	111.3(3)
Re–Sb(1)–C(31)	117.4(3)	Re–Sb(2)–C(61)	125.9(3)
C(11)–Sb(1)–C(21)	97.8(5)	C(41)–Sb(2)–C(51)	97.0(4)
C(11)–Sb(1)–C(31)	104.2(4)	C(41)–Sb(2)–C(61)	105.7(4)
C(21)–Sb(1)–C(31)	98.1(4)	C(51)–Sb(2)–C(61)	97.9(4)
Re–C–O	176(1)–178(1)		

similar pattern to that of *ax*-[$Mn_2(CO)_9(SbPh_3)$]. The complex is poorly soluble in *n*-hexane, but easily dissolves in chlorocarbons.

Reaction of [$Mn(CO)_5Br$] with Ag[CF_3SO_3] and $SbPh_3$ in CH_2Cl_2 produced the carbonyl cation [$Mn(CO)_5(SbPh_3)$][CF_3SO_3]. The [$Mn(CO)_5(SbPh_3)$]ClO_4 complex has been described previously [15]. The pentacarbonyl cation (C_{4v}) is easily identified by three CO stretches at 2135(m), 2060(sh), 2050(s) cm^{-1}, and its structure was confirmed by an X-ray study.

The structure consists of discrete octahedral cations (Fig. 2, Table 1) with Mn–Sb 2.596(3) Å longer (0.07 Å) than in [$Mn_2(CO)_9(SbPh_3)$]. The Mn–C trans to the Sb atom is shorter than the four remaining equatorial distances but unlike the earlier dimetallic compound the Sb–Mn–C(eq) angles do not show the same trend and are close to 90°. It has been noted before in $BiPh_3$ complexes that the C–Bi–C angle increases on coordination but with the effect less for lighter Group 15 ligands [16]. In the present examples the same trend can be observed. In solid $SbPh_3$ the C–Sb–C angle ranges from 95.1(3)–98.0(3), 96.3° (av) [17], whereas in the two manganese complexes reported here the values are 98.6(2)–99.9(2), 99.2° (av) and 101.0(3)–105.4(3), 103.1° (av) (Table 1) with the larger values being in the cationic species.

Manganese carbonyl halides *cis*-$[Mn(CO)_4XL]$ and *mer*, *trans*-$[Mn(CO)_3XL_2]$ ($X = Cl$, Br or I; $L = PR_3$, AsR_3, etc) are well known [1]. In the case of $SbPh_3$ only the bromides are at all well characterised [18,19]. We have prepared three carbonyl chloride complexes. The reaction of $[Mn(CO)_5Cl]$ with $SbPh_3$ in $CHCl_3$ at room temperature produced orange *cis*-$[Mn(CO)_4Cl(SbPh_3)]$, the structure [*III*] following from the three ν(CO) modes in the IR spectrum (theory 4, the *trans* isomer should have two, of which one will be of very low intensity) [18]. Reacting $[Mn(CO)_5Cl]$ with two equivalents of $SbPh_3$ under reflux in $CHCl_3$ produced the orange-yellow *fac*-$[Mn(CO)_3Cl(SbPh_3)_2]$ which shows three ν(CO) stretches consistent with the C_s structure [*IV*]. The isolation of *fac* isomers is unusual with monodentate Group 15 ligands [1], although the corresponding bromide is known [19]. On heating in solution, the *fac* isomer partially converts to the orange *mer*,*trans*-$[Mn(CO)_3Cl(SbPh_3)_2]$ [*V*], which separates first on concentrating the solution. The residual *fac*-$[Mn(CO)_3Cl(SbPh_3)_2]$ can be recovered from the filtrate after removal of the solid *mer*, *trans* isomer. No other products were detected by IR spectroscopy of the solutions. The *mer*,*trans*-$[Mn(CO)_3Cl(SbPh_3)_2]$ exhibits only two ν(CO) IR active modes (theory 3) [19]. A crystal of *mer*,*trans*-$[Mn(CO)_3Cl(SbPh_3)_2]$ was grown from CH_2Cl_2 solution by evaporation, but due to disorder between the CO/Cl groups the structure was not satisfactorily refined. Nonetheless the *trans*-$SbPh_3$ groups were clearly established [20]. An essentially identical crystallographic problem was found in $[Re(NO)_2Cl_2(SbPh_3)_2]$ [21]; the cell dimensions were very similar and again the unusual Z of three was found in space group $P\bar{1}$ with one molecule in a general position and one positioned with the Re atom on a centre of symmetry. The stereochemistry showed *trans* Sb atoms and *cis* Cl atoms in the general position molecule but NO/Cl disorder in the centrosymmetric molecule. As noted above in the neutral carbonyl complexes, the δ(CO) resonances in the $^{13}C\{^1H\}$ NMR spectra are less useful in determining stereochemistry in these complexes due to the small chemical shift range observed and the broadening caused by the ^{55}Mn quadrupole moment (Scheme 1).

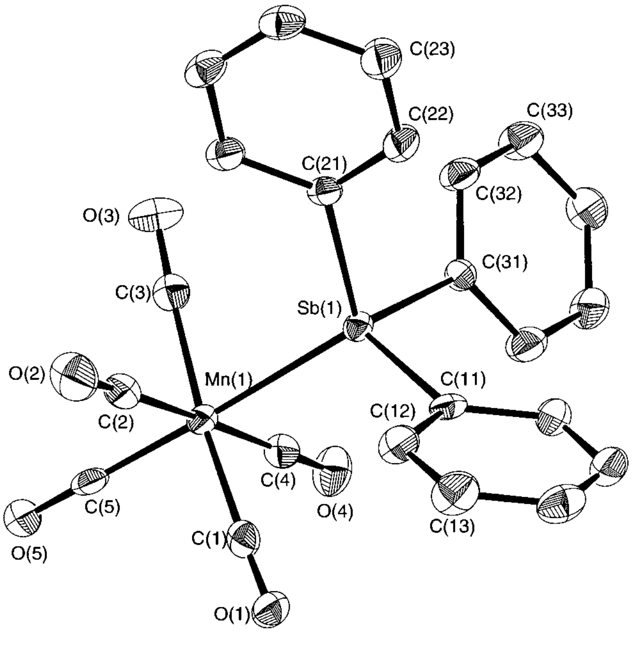

Fig. 2. Structure of the cation in $[Mn(CO)_5(SbPh_3)][CF_3SO_3]$ showing the atom labeling scheme. Displacement ellipsoids are drawn at the 50% probability level and H atoms excluded for clarity.

The corresponding *cis*-$[Re(CO)_4Cl(SbPh_3)]$ and *fac*-$[Re(CO)_3Cl(SbPh_3)_2]$ were made by similar methods to those used for the manganese analogues, although the rates of substitution are very markedly slower. The isomers present were identified from the carbonyl vibrations in the IR spectra (Section 3). However *fac*-$[Re(CO)_3Cl(SbPh_3)_2]$ showed no evidence for isomerisation into the *mer*,*trans* form after 48 h. reflux in $CHCl_3$, as monitored via the IR spectrum of the solution. Comparison of our IR data with Moedritzer's data [22] for the carbonyl iodide analogues shows only very small differences in ν(CO) on changing the halogen. The structure of *fac*-$[Re(CO)_3Cl(SbPh_3)_2]$ was confirmed by a crystal structure determination and the molecule is shown in Fig. 3 with selected bond lengths in Table 1. The octahedral Re geometry shows the expected small angular distortions with Sb(1)–Re–Sb(2) being the largest angle (95.73(3)°). There are very few Re–Sb distances reported in the Cambridge structural database with $[Re(NO)_2Cl_2(SbPh_3)_2]$ [21] being the closest chemical example (Re–Sb 2.711(8), 2.710(8) Å) and showing similar bond lengths to the present compound. As commented on earlier for the Mn compounds, the C–Sb–C angles (97.0(4)–105.7(4), 100.1° (av)) are larger than in the free ligand.

Both naturally occuring rhenium isotopes (^{185}Re and ^{187}Re) have $I = 5/2$ but these are associated with very large quadrupole moments which make them unsuitable for NMR investigation of rhenium complexes. In contrast, ^{55}Mn is a very sensitive NMR nucleus ($I = 5/2$, 100%, $\Xi = 24.66$, $D_c = 994$), but probably due to the moderate quadrupole moment ($Q = 0.55 \times 10^{-28}$ m^2), has been relatively little used [11,23]. Table 2 lists the ^{55}Mn chemical shifts for a range of stibine complexes and Fig. 4 shows the spectrum of $[Mn_2(CO)_9(SbPh_3)]$. The spectra are mostly obtainable in a few minutes, although those containing very broad resonances need

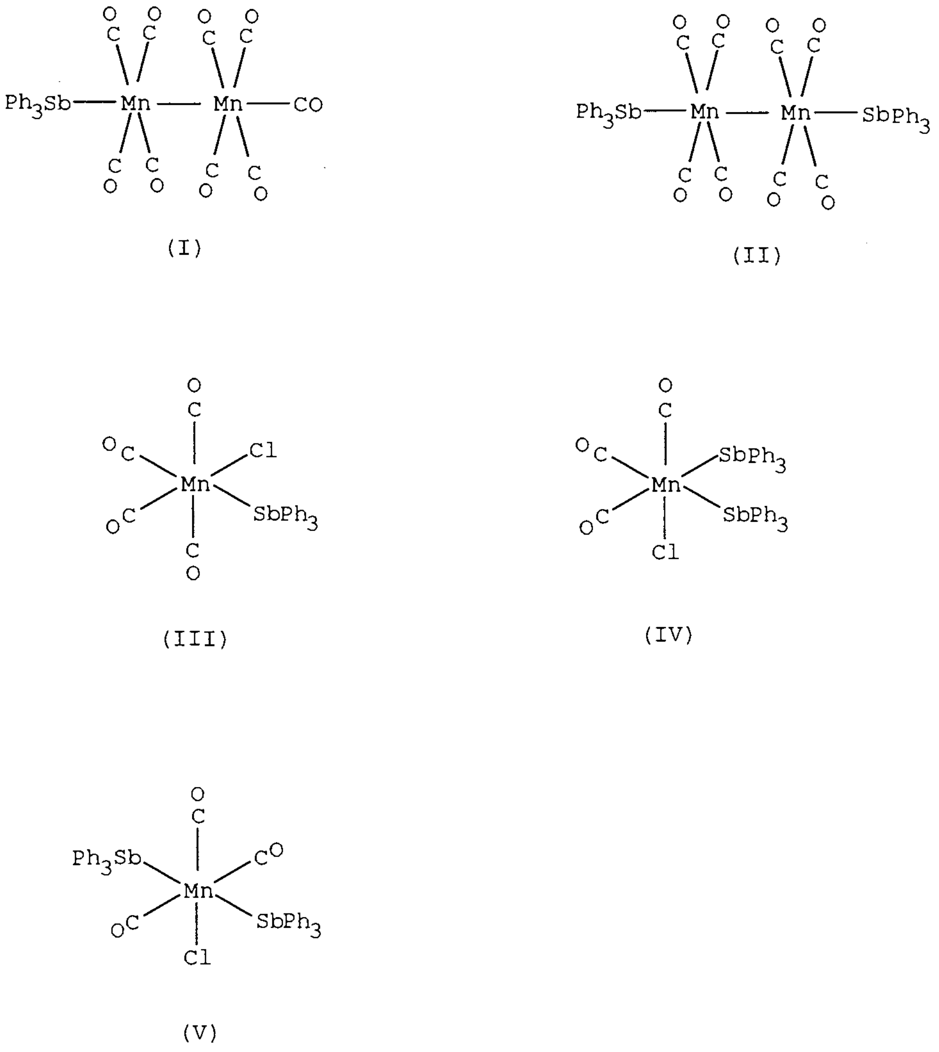

Scheme 1.

somewhat longer. As can be seen for the $SbPh_3$ complexes described above, the δ(Mn) values span ca. 1700 ppm, and this wide chemical shift range coupled with short acquisition times, makes the identification of the components of mixtures straightforward, for example the $[Mn(CO)_{5-x}Cl(SbPh_3)_x]$. As would be expected from the size of the quadrupole, the line widths in the ^{55}Mn spectra are very sensitive to the electric field gradients at the manganese (Table 2), varying from a few hundred Hz to ca. 20000 Hz. Overall ^{55}Mn NMR proves to be a very sensitive probe and merits more widespread use.

2.1. Some comparisons

The reactions of excess PR_3 or AsR_3 (L) with $[Mn_2(CO)_{10}]$ or $[Re_2(CO)_{10}]$ either thermally or photochemically result predominantly in the disubstituted complexes $[M_2(CO)_8L_2]$, and even with stoichiometric amounts of ligand and decacarbonyl, the products are usually mixtures of $[Mn_2(CO)_{10-x}(L)_x]$ ($x = 0$, 1 or 2) separable chromatographically [1]. In contrast, with $SbPh_3$ monosubstitution is favoured irrespective of the $SbPh_3$:$M_2(CO)_{10}$ ratio under both photochemical and amine oxide promoted conditions, and we have not observed any $[Re_2(CO)_8(SbPh_3)_2]$ formation. Thermal substitution of the decacarbonyls with $SbPh_3$ is not a satisfactory route, again contrasting with results in the PR_3 systems. These results largely parallel our previous studies with $Ph_2SbCH_2SbPh_2$ [9] which identified lower levels of CO-substitution and poor yields compared with the analogous diphosphine systems. In the carbonyl halide systems, the isolation of *fac*-$[Mn(CO)_3Cl(SbPh_3)_2]$ which slowly isomerises on heating, compared to the formation of only *mer*,*trans*-isomers with most PR_3 or AsR_3 is also notable. These results suggest that other stibine complexes merit a detailed re-examination; in much of the earlier work, the $SbPh_3$ complexes received cursory mention and often incomplete characterisation in papers focusing on

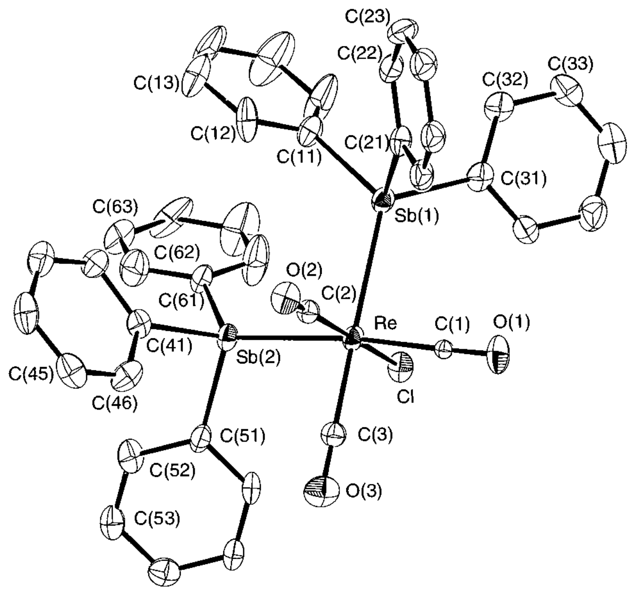

Fig. 3. Molecular structure of $[Re(CO)_3Cl(SbPh_3)_2]$ showing the atom labeling scheme. Displacement ellipsoids are drawn at the 50% probability level and H atoms are excluded for clarity.

phosphine and arsine analogues. It is becoming clear that there are significant differences between SbR_3 and the lighter ligand analogues in many systems [24].

3. Experimental

Physical measurements were made as described elsewhere [9]. ^1H and $^{13}C\{^1H\}$ NMR chemical shifts are quoted relative to TMS; ^{55}Mn chemical shifts are relative to external aqueous $KMnO_4$ solution ($\delta = 0$).

Table 2
^{55}Mn NMR spectroscopic data[a]

Complex	$\delta(^{55}Mn)$	$w_{\frac{1}{2}}$ (Hz)	Reference
$Mn_2(CO)_{10}$	−2325	83	[11]
$[Mn_2(CO)_9(SbPh_3)]$	−2389, −2394	320, 650	This work
$[Mn_2(CO)_8(SbPh_3)_2]$	−2070	14 000	This work
$[Mn_2(CO)_8(\mu\text{-dpsm})]$[b]	−2195	20 000	[9]
$[Mn(CO)_5(SbPh_3)]$-$[CF_3SO_3]$	−1825	3800	This work
$[Mn(CO)_5Cl]$	−1004	331	[11]
$[Mn(CO)_4Cl(SbPh_3)]$	−997	4000	This work
$[Mn(CO)_4Cl(\eta^1\text{-dpsm})]$	−1277	5000	[9]
fac-$[Mn(CO)_3Cl$-$(SbPh_3)_2]$	−730	1000	This work
mer,trans-$[Mn(CO)_3$-$Cl(SbPh_3)_2]$	−920	15 000	This work

[a] Chemical shifts relative to external aqueous $KMnO_4$.
[b] dpsm, $Ph_2SbCH_2SbPh_2$.

3.1. Synthesis

$[Mn_2(CO)_9(SbPh_3)]\cdot[Mn_2(CO)_{10}]$ (0.81 g, 2.1 mmol), $SbPh_3$ (2.1 g, 5.9 mmol) and Me_3NO (0.31 g, 4.1 mmol) were stirred together in toluene (30 ml) under nitrogen at 40°C overnight in an attempt to produce $[Mn_2(CO)_8(SbPh_3)_2]$. The solvent was then removed and the residue adsorbed onto silica. The mixture was chromatographed on silica using *n*-hexane and the first two bands collected, the first being unreacted $[Mn_2(CO)_{10}]$ and the second $[Mn_2(CO)_9(SbPh_3)]$. The volume of *n*-hexane in the second fraction was reduced to ca. 5 ml and the solution placed in the freezer for 2 h to yield orange-brown crystals. Yield 0.30 g, 22%. (Found: C, 45.2; H, 2.0. $C_{27}H_{15}Mn_2O_9Sb$ requires C, 45.3; H, 2.1%). FAB MS (3-NOBA) M^+ 686, 602, 519, 491, 462, 407. Anal. calc. for $[Mn_2(CO)_8(^{121}SbPh_3)]^+$ 686, $[Mn_2(CO)_5(^{121}SbPh_3)]^+$ 602, $[Mn(CO)_4(^{121}SbPh_3)]^+$ 519, $[Mn(CO)_3(^{121}SbPh_3)]^+$ 491, $[Mn(CO)_2(^{121}SbPh_3)]^+$ 463, $[Mn(^{121}SbPh_3)]^+$407. IR: Solution (hexane) 2089 (m), 2010 (m), 1995 (s), 1974 (m), 1937 (m); Nujol mull 2088 (m), 2008 (m), 1993 (s), 1980 (sh), 1936 (m) cm^{-1}. ^1H NMR ($CDCl_3$) 7.2–7.6 (m). $^{13}C\{^1H\}$ NMR ($CDCl_3$) 224.2, 223.5, 135–129.

$[Mn_2(CO)_8(SbPh_3)_2]$. A solution of $[Mn_2(CO)_{10}]$ (2.0 g, 5.13 mmol) and $SbPh_3$ (4.0 g, 11.3 mmol) in toluene (80 ml) was irradiated with UV light (370 nm) under nitrogen with stirring for 12 h. The dark red solution obtained was filtered, and the solvent removed to give a red-brown oil, which was chromatographed in silica using *n*-hexane to give firstly $[Mn_2(CO)_{10}]$ followed by $[Mn_2(CO)_9(SbPh_3)]$ and on switching to dichloromethane as the eluant $[Mn_2(CO)_8(SbPh_3)_2]\cdot CH_2Cl_2$. (Found: C, 47.6; H, 2.9. $C_{45}H_{32}Cl_2Mn_2O_8Sb_2$ requires C, 48.0; H, 2.8%). IR: Solution (dichloromethane) 1977 (br); Nujol mull 1970 (br) cm^{-1}. ^1H NMR ($CDCl_3$) 7.2–7.6, 5.3 (CH_2Cl_2). $^{13}C\{^1H\}$ NMR ($CDCl_3/CH_2Cl_2$) 216.6, 135–128.

$[Mn(CO)_5(SbPh_3)][CF_3SO_3]\cdot[Mn(CO)_5Br]$ (0.337 g, 1.23 mmol) and $AgCF_3SO_3$ (0.47 g, 1.84 mmol) in dichloromethane (50 ml) were stirred together under nitrogen with the exclusion of light for 3 h. The mixture was filtered (Schlenk) and the yellow filtrate stirred with $SbPh_3$ (1.3 g, 3.7 mmol) for a further 3 h. The volume was reduced to ca. 10 ml and *n*-hexane (30 ml) added. The yellow solid produced was filtered off, washed with *n*-hexane (3 × 10 ml) and dried in vacuo. Yield 0.25 g, 29%. (Found: C, 41.5; H, 2.0. $C_{24}H_{15}F_3MnO_8SSb$ requires C, 41.3; H, 2.2%). ES MS (MeCN) M^+ 547, 519, 491, 407, anal. calc. for $[Mn(CO)_5(^{121}SbPh_3)]^+$ 547, $[Mn(CO)_4(^{121}SbPh_3)]^+$ 519, $[Mn(CO)_3(^{121}SbPh_3)]^+$ 491, $[Mn(^{121}SbPh_3)]^+$ 407. IR: Solution (dichloromethane) 2135 (m), 2060(sh), 2050 (s); Nujol mull 2135 (m), 2051 (m) cm^{-1}. ^1H NMR ($CDCl_3$) 7.3–7.7. $^{13}C\{^1H\}$ NMR ($CDCl_3$) 206.4(sh), 205.3, 137–126.

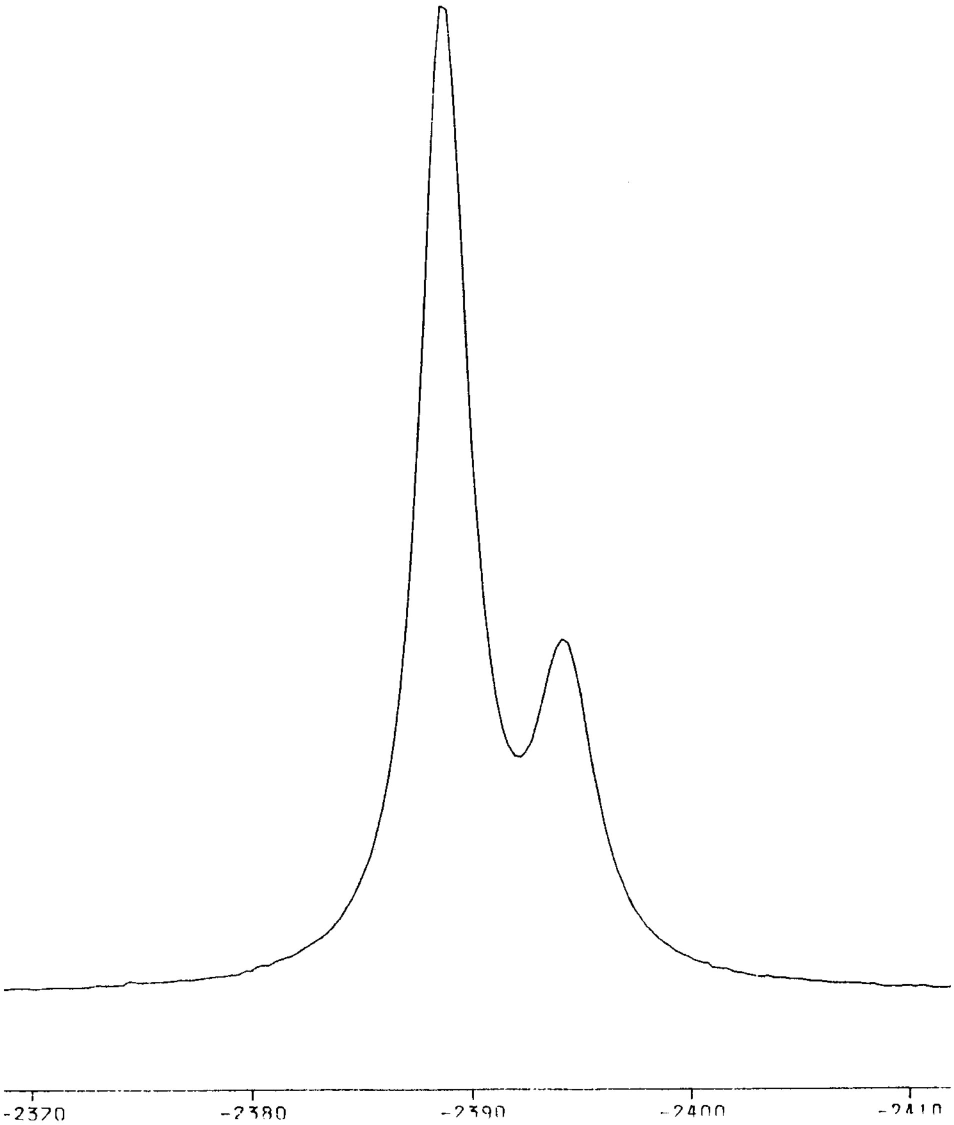

Fig. 4. ^{55}Mn NMR spectrum of $[Mn_2(CO)_9(SbPh_3)]$ in $CHCl_3/CDCl_3$.

$[Mn(CO)_4Cl(SbPh_3)]\cdot[Mn(CO)_5Cl]$ (0.12 g, 0.52 mmol) and $SbPh_3$ (0.18 g, 0.51 mmol) were stirred together under nitrogen in chloroform (10 ml) for 24 h to give an orange solution. The solution was filtered and the solvent removed from the filtrate to give an orange solid. Yield 0.27 g, 92%. (Found: C, 47.5; H, 2.7. $C_{22}H_{15}ClMnO_4Sb$ requires C, 47.5; H, 2.6%). FAB MS (3-NOBA) M^+ 519, 491, 444, 407, anal. calc. for $[Mn(CO)_4(^{121}SbPh_3)]^+$ 519, $[Mn(CO)_3(^{121}SbPh_3)]^+$ 491, $[Mn^{35}Cl(^{121}SbPh_3)]^+$ 442, $[Mn(^{121}SbPh_3)]^+$, 407. IR: Solution (chloroform) 2090 (m), 2012 (s), 1960 (m); Nujol mull 2087 (s), 2002 (s), 1950 (s) cm^{-1}. ^1H NMR ($CDCl_3$) 7.3–7.7. $^{13}C\{^1H\}$ NMR ($CDCl_3$) 215.5, 213.0(sh), 212.5, 136–130.

fac-$[Mn(CO)_3Cl(SbPh_3)_2]\cdot[Mn(CO)_5Cl]$ (0.10 g, 0.43 mmol) and $SbPh_3$ (0.31 g, 0.88 mmol) in chloroform (30 ml) were refluxed together under nitrogen for 24 h. The mixture was then cooled and filtered and the filtrate reduced in volume to ca. 2 ml. Hexane (40 ml) was added and the yellow-orange solid produced was filtered off, washed with hexane (2 × 10 ml) and dried in vacuo. Yield 0.05 g, 13%. (Found: C, 53.3; H, 3.4. $C_{39}H_{30}ClMnO_3Sb_2$ requires C, 53.2; H, 3.4%). FAB MS (3-NOBA) M^+ 845, 796, 761, 444, 407, anal. calc. for $[Mn(CO)_3(^{121}SbPh_3)_2]^+$ 845, $[Mn^{35}Cl(^{121}SbPh_3)_2]^+$ 794, $[Mn(^{121}SbPh_3)_2]^+$ 759, $[Mn^{35}Cl(^{121}SbPh_3)]^+$ 442, $[Mn(^{121}SbPh_3)]^+$ 407. IR: Solution (dichloromethane) 2024 (s), 1955 (m), 1912 (m); Nujol mull 2019 (s), 1954 (s), 1904 (m) cm^{-1}. ^1H NMR ($CDCl_3$) 7.2–7.7. $^{13}C\{^1H\}$ NMR ($CDCl_3$) 211.5, 206.0, 139–127.

mer, *trans*-$[Mn(CO)_3Cl(SbPh_3)_2]\cdot[Mn(CO)_5Cl]$ (0.10 g, 0.43 mmol) and $SbPh_3$ (0.31 g, 0.88 mmol) in chloroform (30 ml) were refluxed together under nitrogen for 22 h. The mixture was then cooled and filtered and the filtrate reduced in volume to ca. 2 ml. Hexane was added and the orange solid produced was filtered off

Table 3
Crystal data for $[Mn_2(CO)_9(SbPh_3)]$, $[Mn(CO)_5(SbPh_3)][CF_3SO_3]$ and $[Re(CO)_3Cl(SbPh_3)_2]$

Compound	$[Mn_2(CO)_9(SbPh_3)]$	$[Mn(CO)_5(SbPh_3)]$-$[CF_3SO_3]$	$[Re(CO)_3Cl(SbPh_3)_2]$
Molecular formula	$C_{27}H_{15}Mn_2O_9Sb$	$C_{24}H_{15}F_3MnO_8SSb$	$C_{39}H_{30}ClO_3ReSb_2$
M_r	715.03	697.12	1011.82
Crystal system	Triclinic	Monoclinic	Orthorhombic
Space group	$P\bar{1}$ (no. 2)	$P2_1/c$ (no. 14)	*Pbca* (no. 61)
a (Å)	10.143(2)	11.711(11)	19.162(7)
b (Å)	11.782(5)	14.705(16)	20.765(10)
c (Å)	13.266(2)	15.115(9)	17.646(16)
α (°)	66.37(1)	90.0	90.0
β (°)	75.20(1)	93.45(6)	90.0
γ (°)	85.84(2)	90.0	90.0
V (Å^3)	1403.4(7)	2598.3(3.7)	7021.3(6.8)
Z	2	4	8
D_{calc} (g cm^{-3})	1.692	1.782	1.914
2 Theta range for cell (°)	—	33.0–38.6	44.2–49.1
Temperature (K)	150	150	150
$F(000)$ (e)	700	1368	3856
Crystal size (mm)	$0.20\times0.18\times0.16$	$0.40\times0.20\times0.07$	$0.40\times0.33\times0.20$
Scan mode	Area detector	ω-2θ	ω-2θ
Total no. of observations	4931	5013	6801
No. of unique observations	3803 ($R_{int}=0.057$)	4769 ($R_{int}=0.0197$)	6184
hkl range	−11 to 9, −13 to 13, −15 to 13	0−13, 0−17, −17 to 17	0−22, 0−24, 0−20
Absorption correction	None	None	Analytical
Max/min transmission	—,—	—,—	0.361,0.227
No. of data in refinement	3803	3808 ($F>4\sigma(F)$)	6184
No. of parameters/restraints	262/0	338/0	401/36
Weighting scheme (w^{-1})	$\sigma^2(Fo^2)$	$\sigma^2(Fo^2)$	$\sigma^2(Fo^2)+(0.18P)^2+(5.08P)$ $P=(F_o^2+2F_c^2)/3$
λ (Å) (Mo–K$_\alpha$)	0.71073	0.71073	0.71073
μ (cm^{-1})	18.9	16.55	50.8
Max 2θ (°)	49.5	50.0	50.0
S	0.47	3.15	1.09
Max shift (esd)	0.04	0.01	−0.10
Residual electron density (eÅ^{-3})	−0.715 to +0.675	−1.99 to +1.53	−5.81 to +3.05
R ($F>n\sigma(F)$)	0.041 ($n=4$, 2669 refs.)	0.048 ($n=4$, 3808 refs.)	0.062 ($n=4$, 4942 refs.)
R (all data)	0.049	—	0.081
wR_2 (all data)	0.130	—	0.225
wR ($F>n\sigma(F)$)	—	0.057 ($n=4$, 3808 refs.)	—

$[R=\Sigma||Fo|-|Fc||/\Sigma|Fo|;\ wR_2=[\Sigma w(Fo^2-Fc^2)^2/\Sigma wFo^4]^{\frac{1}{2}};\ wR=[\Sigma w(Fo-Fc)^2/\Sigma wFo^2]^{\frac{1}{2}}.$

and by solution IR was shown to be a mixture of *fac*-$[Mn(CO)_3Cl(SbPh_3)_2]$ and $[Mn(CO)_4Cl(SbPh_3)]$. The solid was refluxed with more $SbPh_3$ (0.10 g, 0.28 mmol) in chloroform for a further 2 h. On cooling hexane (20 ml) was added and the mixture reduced in volume until an orange solid precipitated *mer*,*trans*-$[Mn(CO)_3Cl(SbPh_3)_2]$. This was filtered off and washed with hexane. The yellow filtrate was reduced in volume further to yield a yellow-orange solid*fac*-$[Mn(CO)_3Cl(SbPh_3)_2]$ this was also filtered off and washed with hexane. (Found: (*mer*,*trans)* C, 53.5; H, 3.3. $C_{39}H_{30}ClMnO_3Sb_2$ requires C, 53.2; H, 3.4%). FAB MS (3-NOBA) 880, 845, 796, 761, 444, anal. calc. for $[Mn(CO)_3^{35}Cl(^{121}SbPh_3)_2]^+$ 878, $[Mn(CO)_3(^{121}SbPh_3)_2]^+$ 843, $[Mn^{35}Cl(^{121}SbPh_3)_2]^+$ 794, $[Mn(^{121}SbPh_3)_2]^+$ 759, $[Mn^{35}Cl(^{121}SbPh_3)]^+$ 442. IR: Solution (dichloromethane) 1950 (s), 1909 (m); Nujol mull 1942 (s), 1893 (s) cm^{-1}. ^1H NMR ($CDCl_3$) 7.2–7.7. $^{13}C\{^1\}$ NMR ($CDCl_3$) 221.7, 219.8, 137–127.

$[Re_2(CO)_9(SbPh_3)]\cdot[Re_2(CO)_{10}]$ (0.50 g, 0.77 mmol) and $SbPh_3$ (0.54 g, 1.54 mmol) in degassed toluene (40 ml) were irradiated under nitrogen with stirring overnight. The mixture was then adsorbed onto alumina and eluted with dichloromethane-*n*-hexane (1:3) to give $[Re_2(CO)_{10}]$ (first band collected —colourless) and $[Re_2(CO)_9(SbPh_3)]$ (second band collected—yellow). The solvent was removed from the collected fractions and the residue recrystallised from CH_2Cl_2-hexane to give a yellow solid. This was filtered, washed with hexane (2×10 ml) and dried in vacuo. Yield 0.1 g, 13%. (Found: C, 32.9; H, 1.7. $C_{27}H_{15}O_9Re_2Sb$ requires C, 33.2; H, 1.5%). FAB MS (3-NOBA) 974, 948, 925, 893, 869, 623, 567, 539, anal. calc. for $[^{185}Re_2(CO)_9(^{121}SbPh_3)]^+$ 974, $[^{185}Re_2(CO)_8(^{121}SbPh_3)]^+$

946, $[^{185}Re_2(CO)_7(^{121}SbPh_3)]^+$ 918, $[^{185}Re_2(CO)_6(^{121}SbPh_3)]^+$ 890, $[^{185}Re_2(CO)_5(^{121}SbPh_3)]^+$ 862, $[^{185}Re_2(CO)_9]^+$ 622, $[^{185}Re(CO)(^{121}SbPh_3)]^+$ 565, $[^{185}Re(^{121}SbPh_3)]^+$ 537. ^1H NMR ($CDCl_3$) 7.1–7.5. $^{13}C\{^1H\}$ NMR ($CDCl_3$) 193.0, 190.3, 188.2, 136–127. IR: Solution (dichloromethane) 2086 (w), 2009 (sh), 1996 (s), 1971 (s), 1925 (m); Nujol mull 2082 (m), 2008 (sh), 1994 (s), 1978 (s), 1925 (s) cm^{-1}.

$[Re(CO)_4Cl(SbPh_3)]\cdot[Re(CO)_5Cl]$ (0.066 g, 0.18 mmol) and $SbPh_3$ (0.064 g, 0.18 mmol) were refluxed in chloroform (30 ml) for 2 h. On cooling *n*-hexane (25 ml) was added and on reducing the volume a white solid obtained. This was filtered off, washed with hexane (2 × 10 ml) and dried in vacuo. Yield 0.080 g, 65%. (Found: C, 38.6; H, 2.3. $C_{22}H_{15}ClO_4ReSb$ requires C, 38.5; H,2.2%). FAB MS (3-NOBA) 687, 651, 623. Anal. calc. for $[^{185}Re^{35}Cl(CO)_4(^{121}SbPh_3)]^+$ 684, $[^{185}Re(CO)_4(^{121}SbPh_3)]^+$ 649, $[^{185}Re(CO)_3(^{121}SbPh_3)]^+$ 621. ^1H NMR ($CDCl_3$) 7.3–7.6. $^{13}C\{^1H\}$ NMR ($CDCl_3$) 186.0, 182.7, 182.4, 136–129. IR: Solution (chloroform) 2107 (m), 2013 (s), 1947 (m); Nujol mull 2103 (m), 1997 (s), 1936 (s) cm^{-1}.

Table 4
Atomic coordinates and equivalent displacement parameter ($Å^2 \times 10^3$) for $[Mn_2(CO)_9(SbPh_3)]$

Atom	x	y	z	U_{eq}
Sb(1)	0.24203(4)	0.83866(3)	0.83696(3)	16(1)
Mn(1)	0.42107(10)	0.72969(8)	0.74050(7)	16(1)
Mn(2)	0.62891(11)	0.59879(8)	0.63684(8)	20(1)
O(1)	0.5923(5)	0.9611(4)	0.5825(4)	34(1)
O(2)	0.5985(5)	0.6930(4)	0.9016(4)	31(1)
O(3)	0.2877(5)	0.4774(4)	0.8860(4)	31(1)
O(4)	0.2625(6)	0.7580(5)	0.5679(5)	43(1)
O(5)	0.8453(6)	0.7473(5)	0.6570(5)	43(1)
O(6)	0.6191(5)	0.4225(4)	0.8772(4)	32(1)
O(7)	0.3883(6)	0.4673(4)	0.6294(4)	36(1)
O(8)	0.6065(6)	0.8037(5)	0.4158(4)	47(2)
O(9)	0.8305(6)	0.4575(5)	0.5320(4)	41(1)
C(1)	0.5250(7)	0.8731(6)	0.6428(5)	22(2)
C(2)	0.5300(7)	0.7059(5)	0.8406(5)	19(2)
C(3)	0.3379(7)	0.5741(6)	0.8308(6)	22(2)
C(4)	0.3249(8)	0.7462(6)	0.6338(6)	25(2)
C(5)	0.7618(8)	0.6938(6)	0.6482(6)	28(2)
C(6)	0.6210(7)	0.4895(6)	0.7855(6)	21(2)
C(7)	0.4804(8)	0.5174(6)	0.6337(5)	25(2)
C(8)	0.6137(8	0.7264(6)	0.4988(6)	30(2)
C(9)	0.7530(8)	0.5119(6)	0.5724(6)	28(2)
C(11)	0.0667(7)	0.9154(5)	0.7707(5)	20(1)
C(12)	0.0827(7)	0.9924(6)	0.6549(6)	27(2)
C(13)	−0.0287(8)	1.0520(6)	0.6151(6)	30(2)
C(14)	−0.1598(8)	1.0331(6)	0.6910(6)	32(2)
C(15)	−0.1764(8)	0.9547(6)	0.8063(6)	34(2)
C(16)	−0.0637(7)	0.8955(6)	0.8461(6)	25(2)
C(21)	0.1419(7)	0.7353(5)	1.0118(5)	20(1)
C(22)	0.1361(7)	0.7818(6)	1.0949(6)	24(2)
C(23)	0.0754(8)	0.7103(6)	1.2094(6)	30(2)
C(24)	0.0215(8)	0.5893(6)	1.2423(6)	33(2)
C(25)	0.0257(8)	0.5425(6)	1.1598(6)	29(2)
C(26)	0.0858(7)	0.6147(6)	1.0441(6)	26(2)
C(31)	0.3087(7)	0.9993(5)	0.8510(5)	18(1)
C(32)	0.4455(8)	1.0085(6)	0.8541(6)	30(2)
C(33)	0.4896(8)	1.1149(6)	0.8656(6)	38(2)
C(34)	0.3963(7)	1.2070(6)	0.8718(6)	27(2)
C(35)	0.2615(7)	1.1980(6)	0.8660(5)	23(2)
C(36)	0.2177(7)	1.0930(5)	0.8565(5)	22(2)

Table 5
Atomic coordinates and equivalent displacement parameter ($Å^2$) for $[Mn(CO)_5(SbPh_3)][CF_3SO_3]$

Atom	x	y	z	B_{eq}
Sb(1)	0.17077(4)	0.16551(3)	0.88699(3)	1.42(1)
Mn(1)	−0.04881(9)	0.18946(7)	0.88787(7)	1.54(2)
S(1)	0.7242(2)	0.2202(1)	0.6093(1)	1.84(4)
F(1)	0.5268(5)	0.1868(5)	0.6741(5)	6.4(2)
F(2)	0.5940(5)	0.3185(4)	0.7062(3)	4.6(1)
F(3)	0.5221(5)	0.2918(4)	0.5750(4)	5.3(2)
O(1)	−0.0492(4)	0.0717(3)	1.0502(3)	2.3(1)
O(2)	−0.0205(5)	0.3487(4)	1.0122(4)	3.5(1)
O(3)	−0.0147(5)	0.3052(4)	0.7280(4)	2.9(1)
O(4)	−0.0771(5)	0.0241(4)	0.7710(4)	2.7(1)
O(5)	−0.3034(4)	0.2159(4)	0.8748(3)	2.2(1)
O(6)	0.7755(5)	0.1787(4)	0.6883(3)	2.7(1)
O(7)	0.7766(5)	0.3039(4)	0.5844(4)	3.1(1)
O(8)	0.6970(5)	0.1587(4)	0.5372(3)	2.7(1)
C(1)	−0.0510(6)	0.1165(5)	0.9894(5)	1.9(2)
C(2)	−0.0294(6)	0.2899(5)	0.9654(5)	2.1(2)
C(3)	−0.0311(6)	0.2618(5)	0.7869(5)	1.9(2)
C(4)	−0.0677(6)	0.0873(5)	0.8140(5)	2.2(2)
C(5)	−0.2068(7)	0.2060(5)	0.8810(5)	1.8(2)
C(11)	0.2537(6)	0.0959(5)	0.9963(4)	1.6(1)
C(12)	0.2392(7)	0.1312(5)	1.0793(5)	2.3(2)
C(13)	0.2959(8)	0.0906(6)	1.1523(5)	2.9(2)
C(14)	0.3660(7)	0.0150(6)	1.1421(5)	2.7(2)
C(15)	0.3782(6)	−0.0195(5)	1.0593(5)	2.5(2)
C(16)	0.3231(6)	0.0206(5)	0.9852(5)	2.1(2)
C(21)	0.2697(6)	0.2868(5)	0.8850(4)	1.5(1)
C(22)	0.3876(6)	0.2808(5)	0.8951(5)	2.2(2)
C(23)	0.4543(7)	0.3585(5)	0.8992(5)	2.6(2)
C(24)	0.4016(7)	0.4438(5)	0.8947(5)	2.3(2)
C(25)	0.2846(7)	0.4502(5)	0.8841(5)	2.2(2)
C(26)	0.2174(6)	0.3727(5)	0.8804(5)	1.9(2)
C(31)	0.2193(6)	0.0953(5)	0.7728(4)	1.5(1)
C(32)	0.2613(7)	0.1428(5)	0.7029(5)	2.1(2)
C(33)	0.2848(7)	0.0991(5)	0.6246(5)	2.5(2)
C(34)	0.2695(7)	0.0057(5)	0.6183(5)	2.5(2)
C(35)	0.2298(7)	−0.0421(5)	0.6874(5)	2.5(2)
C(36)	0.2027(7)	0.0006(5)	0.7649(5)	2.4(2)
C(40)	0.5846(7)	0.2558(6)	0.6421(6)	3.1(2)

fac-$[Re(CO)_3Cl(SbPh_3)_2]\cdot[Re(CO)_5Cl]$ (0.10 g, 0.28 mmol) and $SbPh_3$ (0.21 g, 0.59 mmol) were refluxed in chloroform (30 ml) for 45 h. On cooling the volume was reduced to ca. 5 ml and diethyl ether (20 ml) added to give a light fawn solid. This was filtered off, washed with diethyl ether (2 × 10 ml) and dried in vacuo. Yield 0.15 g, 53%. (Found: C, 46.7; H, 3.1. $C_{39}H_{30}ClO_3ReSb_2$ requires C, 46.3; H, 3.0%). FAB MS (3-NOBA) 1011, 983, 623, 539. Anal. calc. for $[^{185}Re^{35}Cl(CO)_3(^{121}SbPh_3)_2]^+$ 1008, $[^{185}Re^{35}Cl(CO)_2(^{121}SbPh_3)_2]^+$ 980,

$[^{185}Re^{35}Cl(CO)_3(^{121}SbPh_3)]^+$ 621, $[^{185}Re(^{121}SbPh_3)]^+$ 537. ^1H NMR ($CDCl_3$) 7.2–7.5. $^{13}C\{^1H\}$ NMR ($CDCl_3$) 191–186(br), 136–130. IR: Solution (dichloromethane) 2032 (s), 1952 (m), 1906 (m); Nujol mull 2021 (s), 1954 (s), 1926 (s) cm^{-1}.

3.2. Crystallography

Air-stable crystals were obtained from cooling (freezer, −20°C) a hexane solution overnight ($[Mn_2(CO)_9(SbPh_3)]$) and by liquid diffusion of diethyl ether into a dichloromethane solution for the other two compounds. Crystals were mounted on glass fibres using the oil-film technique and held at 150 K using an Oxford Cryosystems low temperature device. Data were recorded using an Enraf-Nonius FAST system ($[Mn_2(CO)_9(SbPh_3)]$ only) and a Rigaku AFC7S both diffractometers being fitted with graphite monochromator and Mo–K_α radiation. For all structures, the heavy atoms were located using SHELXS-86 direct methods [25] and lighter atoms added by repeated structure factor and electron density calculations. No significant decay was noted and no absorption correction was applied to the manganese data. No evidence for the H atom positions appeared in later maps for $[Mn_2(CO)_9(SbPh_3)]$ and they were not included in the model. Full-matrix least-squares refinement on F^2 was carried out using SHELXL-97 [26] with anisotropic (Sb, Mn, O, C (of CO's)) and isotropic (C (phenyl)) thermal displacement parameters. For $[Mn(CO)_5(SbPh_3)][CF_3SO_3]$, all the H atoms appeared in the later electron-density maps and they were added to the model but not refined. For this compound, refinement on F was carried out using the teXsan package [27] with anisotropic thermal displacement parameters for all atoms types (except H). For the rhenium compound, an analytical absorption correction was applied and refinement carried out using SHELXL-97 [26]. Some C atom anisotropic displacement parameters became non-positive definite and the rigid bond approximation was introduced for the phenyl rings (DELU instruction for adjacent atoms). A number of plausible H atoms appeared in later electron density maps and all the H's were introduced into the model in calculated positions ($d(C–H) = 0.95$ Å) with a common refined displacement parameter. The large peak and trough in the difference electron-density map is close to the rhenium (ca. 1 Å) and an alternative ψ-scan absorption correction failed to change matters. These features presumably reflect an inadequate absorption correction. Crystallographic data are summarised in Table 3 and atomic coordinates are given in Tables 4–6. Figs. 1–3 were produced using ORTEP [28].

Table 6
Atomic coordinates and equivalent displacement parameter ($Å^2 \times 10^3$) for $[Re(CO)_3Cl(SbPh_3)_2]$

Atom	x	y	z	U_{eq}
Re	0.09677(2)	0.59561(2)	0.96568(3)	21(1)
Sb(1)	0.11545(4)	0.64721(3)	0.82490(4)	23(1)
Sb(2)	0.23520(4)	0.58573(3)	0.99927(4)	23(1)
Cl	0.10833(15)	0.70647(14)	1.02015(18)	30(1)
O(1)	−0.0622(4)	0.6106(5)	0.9456(6)	39(2)
O(2)	0.0954(4)	0.4615(4)	0.8977(5)	38(2)
O(3)	0.0697(5)	0.5316(4)	1.1202(5)	38(2)
C(1)	−0.0038(5)	0.6035(4)	0.9535(5)	14(2)
C(2)	0.0974(5)	0.5087(5)	0.9213(6)	20(2)
C(3)	0.0811(6)	0.5579(5)	1.0633(6)	24(2)
C(11)	0.2159(6)	0.6572(5)	0.7757(7)	29(2)
C(12)	0.2556(7)	0.6027(6)	0.7636(10)	43(3)
C(13)	0.3229(8)	0.6065(8)	0.7333(10)	57(4)
C(14)	0.3503(8)	0.6672(9)	0.7181(11)	66(5)
C(15)	0.3114(10)	0.7220(8)	0.7304(14)	86(7)
C(16)	0.2446(9)	0.7149(7)	0.7588(13)	72(6)
C(21)	0.0689(6)	0.5917(4)	0.7372(7)	24(2)
C(22)	0.0926(6)	0.5954(5)	0.6623(8)	30(3)
C(23)	0.0617(6)	0.5585(7)	0.6065(7)	36(3)
C(24)	0.0074(6)	0.5181(6)	0.6229(7)	36(3)
C(25)	−0.0172(6)	0.5135(6)	0.6966(7)	33(3)
C(26)	0.0137(6)	0.5505(5)	0.7535(7)	30(2)
C(31)	0.0650(6)	0.7371(5)	0.8012(7)	27(2)
C(32)	0.0692(6)	0.7618(5)	0.7281(7)	30(2)
C(33)	0.0291(7)	0.8159(6)	0.7088(7)	35(3)
C(34)	−0.0119(7)	0.8458(6)	0.7627(9)	41(3)
C(35)	−0.0163(8)	0.8196(7)	0.8354(8)	43(3)
C(36)	0.0232(7)	0.7657(6)	0.8544(7)	35(3)
C(41)	0.2784(6)	0.4918(6)	0.9796(6)	24(2)
C(42)	0.3297(6)	0.4795(5)	0.9239(6)	29(2)
C(43)	0.3533(7)	0.4185(6)	0.9149(8)	39(3)
C(44)	0.3296(7)	0.3675(6)	0.9604(8)	37(3)
C(45)	0.2771(7)	0.3795(6)	1.0130(8)	37(3)
C(46)	0.2533(7)	0.4424(6)	1.0231(7)	34(3)
C(51)	0.2523(6)	0.5883(5)	1.1179(7)	27(2)
C(52)	0.3115(6)	0.5603(5)	1.1485(7)	31(2)
C(53)	0.3229(6)	0.5613(6)	1.2264(7)	34(3)
C(54)	0.2747(7)	0.5899(5)	1.2748(8)	33(3)
C(55)	0.2163(6)	0.6179(5)	1.2440(7)	30(2)
C(56)	0.2056(6)	0.6177(5)	1.1665(7)	29(2)
C(61)	0.3158(6)	0.6534(6)	0.9665(6)	27(2)
C(62)	0.3834(8)	0.6366(7)	0.9692(8)	43(3)
C(63)	0.4344(6)	0.6830(7)	0.9558(7)	36(3)
C(64)	0.4174(7)	0.7451(7)	0.9401(10)	52(4)
C(65)	0.3474(8)	0.7605(7)	0.9375(12)	71(5)
C(66)	0.2950(8)	0.7134(7)	0.9504(11)	61(5)

4. Supplementary material available

Displacement parameters, atomic coordinates, hydrogen atom coordinates, full bond length, angle data and crystallographic data for $[Mn_2(CO)_9(SbPh_3)]$, $[Mn(CO)_5(SbPh_3)][CF_3SO_3]$ and $[Re(CO)_3Cl(SbPh_3)_2]$ have been deposited at the Cambridge Crystallographic Data Centre.

Acknowledgements

We thank the EPSRC for support (NJH) and for funds to purchase the X-ray diffractometer and for access to the Chemical Database Service at the Daresbury Laboratory. We also thank Professor M.B. Hursthouse for data collection on the EPSRC X-ray service Enraf-Nonius FAST diffractometer.

References

[1] (a) P.M. Treichel, in: E.W. Abel, G. Wilkinson, F.G.A. Stone (Eds.), Comprehensive Organometallic Chemistry, Series II, vol. 6, Ch. 1, Pergamon, Oxford, 1995. (b) J.M. O'Connor, in: E.W. Abel, G. Wilkinson, F.G.A. Stone (Eds.), Comprehensive Organometallic Chemistry, Series II, vol. 6, Ch. 6, Pergamon, Oxford, 1995.
[2] W. Hieber, W. Freyer, Chem. Ber. 92 (1959) 1765.
[3] J.R. Miller, D.H. Myers, Inorg. Chim. Acta 5 (1971) 215.
[4] A.G. Osborne, M.H.B. Stiddard, J. Chem. Soc. (1964) 634.
[5] H. Wawersik, F. Basolo, Chem. Commun. (1966) 366.
[6] F.A. Hartman, A. Wojcicki, J. Am. Chem. Soc. 88 (1966) 844.
[7] (a) H.T. Zhang, T.L. Brown, J. Am. Chem. Soc. 115 (1993) 107. (b) S. Zhang, X. Song, T.L. Brown, Organometallics 14 (1995) 2366.
[8] N.A.D. Carey, J.G. Noltes, Chem. Commun. (1968) 1471.
[9] A.M. Hill, W. Levason, M. Webster, I. Albers, Organometallics 16 (1997) 5641.
[10] (a) G.W. Harris, N.J. Coville, J. Crystallogr. Spectros. Res. 19 (1989) 451. (b) R.H. Reimann, E. Singleton, J. Chem. Soc. Dalton Trans. (1976) 2109.
[11] J. Mason (Ed.), Multinuclear NMR, Plenum, New York, 1987.
[12] (a) M.R. Churchill, K.N. Amoh, H.J. Wasserman, Inorg. Chem. 20 (1981) 1609. (b) M. Martin, B. Rees, A. Mitschler, Acta Crystallogr. B38 (1982) 6.
[13] M. Laing, E. Singleton, R. Reimann, J. Organomet. Chem. 56 (1973) C21.
[14] (a) U. Koelle, J. Organomet. Chem. 155 (1978) 53. (b) W.L. Ingham, N.J. Coville, J. Organomet. Chem. 423 (1992) 51.
[15] R. Uson, V. Riera, J. Gimeno, M. Laguna, M.P. Gamasa, J. Chem. Soc. Dalton Trans. (1979) 996.
[16] N.J. Holmes, W. Levason, M. Webster, J. Organomet. Chem. 545–6 (1997) 111.
[17] E.A. Adams, J.W. Kolis, W.T. Pennington, Acta Crystallogr. C46 (1990) 917.
[18] R.J. Angelici, F. Basolo, J. Am. Chem. Soc. 84 (1962) 2495.
[19] A.M. Bond, R. Colton, M.E. McDonald, Inorg. Chem. 17 (1978) 2842.
[20] [$Mn(CO)_3Cl(SbPh_3)_2$]: $C_{39}H_{30}ClMnO_3Sb_2$, $M_r = 880.56$, triclinic, $a = 13.982(8)$, $b = 16.586(11)$, $c = 12.315(8)$ Å, $\alpha = 96.77(5)$, $\beta = 90.21(6)$, $\gamma = 66.71(4)°$, $V = 2602.0(2.9)$ Å^3, T = 150 K, $Z = 3$, $D_x = 1.685$ g cm^{-3}, space group $P\bar{1}$ or $P1$. The linear $MnSb_2$ groups were located by direct methods in space groups $P\bar{1}$ and $P1$, and are all aligned parallel to the c direction. In $P\bar{1}$, one Mn atom is positioned on a centre of symmetry. In both space groups plausible carbon atoms of a number of complete and incomplete phenyl groups were evident but the models failed to refine, probably due to disorder or pseudosymmetry problems. As expected the $P1$ model showed severe correlation.
[21] D. Fenske, N. Mronga, K. Dehnicke, Z. Anorg. Allg. Chem. 498 (1983) 131.
[22] K. Moedritzer, Synth, Inorg. Met. Org. Chem. 2 (1972) 121.
[23] P.S. Pregosin (Ed.), Transition Metal NMR, Elsevier, Amsterdam, 1992.
[24] N.R. Champness, W. Levason, Coord. Chem. Rev. 133 (1994) 115.
[25] G.M. Sheldrick, Acta Crystallogr. A46 (1990) 467.
[26] G.M. Sheldrick, SHELXL-97 Program for Crystal Structure Refinement, University of Göttingen, Germany, 1997.
[27] teXsan, Crystal Structure Analysis Package (version 1.7-1), Molecular Structure Corporation, 3200 Research Forest Drive, The Woodlands, TX 77381, 1995.
[28] C.K. Johnson, ORTEP II, Report ORNL-5138, Oak Ridge National Laboratory, Oak Ridge, TN, 1976.